Development of an energy source management system for a prototype supercapacitor rough terrain mine vehicle

Wilhelm Bisschoff[1], Nima Zabihi[2], and Rupert Gouws[1]
[1]School of Electrical, Electronic and Computer Engineering, North-West University, Potchefstroom Campus, South Africa
Rupert.gouws@nwu.ac.za
[2]International Automotive Research Centre (IARC), WMG, University of Warwick, Coventry, UK
N.Zabihi@warwick.ac.uk

***Abstract*—The mining industry is currently looking to implement electric vehicles into the underground tunnels of mines to reduce the amount of carbon pollution in these tunnels. Electric vehicles offer the benefits of no carbon emissions and less generated heat. The main challenge of an electric vehicle lies in the form of the energy storage system. The energy storage system currently used in electric vehicles consists mainly of large banks of batteries. Batteries have the advantage of being energy dense, which implies that the stored energy can be discharged for an extended period of time. Opposing the energy dense sources is the power dense energy sources. These sources have the capability of discharging all of its stored energy within a short period of time. An example of such an energy source is a supercapacitor. The rough terrain mine vehicle is driven by a supercapacitor bank and a battery connected to an energy source management system, which reaps the advantages of both energy sources.**

Keywords— supercapacitors, lithium-polymer battery, electric vehicle, energy source management

I. INTRODUCTION

In the modern mining industry, the demand for mining support vehicles has increased significantly in order to increase the productivity of mines (Goldwyer, 2007; Topp, 2008). These support vehicles include all of the vehicles that are used to transport tools, mineworkers and extracted materials. Therefore, the support vehicles are responsible for key tasks relating to increased productivity. The large-sized support vehicles, such as dump trucks, excavators etc., are mostly driven by internal combustion engines with the exception of a few hybrid vehicles (HV) implementing an AC electrical drive (Hitachi, 2012).

The core of an electric vehicle lies in the energy source and the power outflow from the source. The energy source which is most widely used as storage medium in an electrical vehicle is a battery (Neenu, 2012). A battery has the characteristic of being very energy dense; this implies that a battery can discharge lower amounts of energy over a long period of time. The opposite of an energy dense source is a power dense energy source. A power dense energy source can instantaneously inject a significant amount of energy into a system. Power density in an energy source is very important in high power applications as this ensures that the energy source does not fall short of supplying the necessary power to the load (Neenu, 2012; Baisden & Emadi, 2004). An energy source that is used to fulfil a power dense demand is a supercapacitor.

Supercapacitors operate in a similar manner as traditional capacitors which store energy inside an electric field. The main difference is that the supercapacitors use double-layer technology which ultimately increases the plate area and decreases the distance between the plates (Maxwell Technologies, 2012). This allows supercapacitors to reach capacitances of up to 3000 F. One of the drawbacks of a supercapacitor is that it has a very low output voltage ranging from only 2.2 to 2.7 V. Another drawback is that the energy density is very low compared to batteries; a supercapacitor with the characteristics mentioned above has an energy density of almost 11000 J. This is equivalent to a single AA lithium-ion battery (Braun et al., 2012). However, the power density of a supercapacitor cannot be matched by any form of battery. An AA lithium-ion battery is able to deliver a continuous current of about 5 A; however, a supercapacitor can continuously deliver currents ranging from 50 A to 220 A (Maxwell Technologies, 2012). This makes the supercapacitor a superior energy source in high power applications. A supercapacitor also has the capability of fully re-charging within a few seconds as opposed to a battery that requires a few hours. A summary of batteries as opposed to supercapacitors is shown in Table 1 (Olivo, 2010; Tuite, 2012; Song et al., 2010).

Table 1: Comparison of supercapacitors and batteries

Supercapacitors	Batteries (General)
Power dense	Energy dense
Short charge time (less than 30 seconds)*	Long charge time (1 to 8 hours)
Expensive initial cost**	Low initial cost
Long lifespan (1 000 000 cycles)	Short lifespan (300-1500 cycles)

*Dependent on current supplying capability
**Price related to 2013

II. Rough Terrain Vehicle Overview

There are four main components of the rough terrain vehicle which include the energy source management system, the control system, the speed/steering control along with the mechanical part of the vehicle and the navigation method. These four individual building blocks are divided into sub-blocks and the overview can be seen in Figure 1. The main focus of the mining vehicle is to effectively use the most effective energy source for supplying the vehicle either from a supercapacitor bank or a battery. The battery is used to supply power to the vehicle in low-to-normal current demanding situations whereas the supercapacitors are used to supply the vehicle in the case of high current demands; i.e. when the vehicle is driving on an incline or is heavily loaded with tools or machinery.

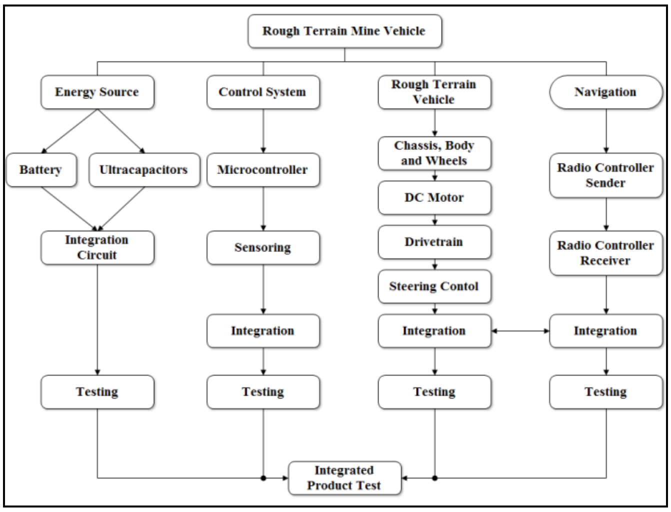

Figure 1: Rough terrain mine vehicle conceptual design

III. Design

The design of the rough terrain mining vehicle consists of four main building blocks as shown in Figure 1; the design thereof is discussed below.

A. *Energy Source DC-DC Converter*

A DC-DC converter is required to connect the battery and supercapacitor bank to the drive and steering motors of the rough terrain vehicle. The DC-DC converter comes in the form of power MOSFET switches acting as pass elements to supply the necessary power to the drive and steering motor. The switching circuit consists of two sets of three parallel connected P-channel power MOSFETs which are controlled by dedicated MOSFET driver circuits. The driver circuits accept low-voltage inputs from the control system; the converter is shown in Figure 2.

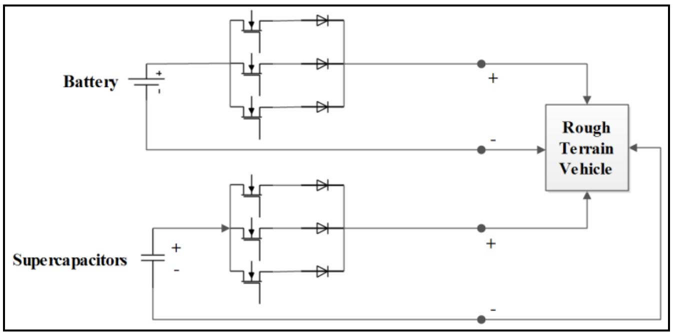

Figure 2: DC-DC converter circuit

Since the battery and supercapacitors share a common positive voltage rail which supplies the vehicle with power, it is required to provide isolation between the energy sources. The diodes prevent the reverse biasing of the P-channel MOSFETs which provides the necessary isolation between the two energy sources. Non-isolated sources will cause passive balancing between the energy sources which may result in component failure and a commonly balanced output voltage (Neenu, 2012).

The supercapacitor bank consists of six 2.7 V, 3000 F series connected supercapacitors to provide a combined voltage of 16.2 V. The continuous current discharging capability of the supercapacitor bank is rated at 130 A at 15 °C and increases to 220 A at 40 °C. The energy storage level of each supercapacitor is rated at 3.0 Wh.

The battery which is used as a support energy source for the supercapacitor bank is lithium-polymer based and has a 4 Ah rating with a nominal voltage of 14.8 V-16.8 V.

B. *Control System*

To reap the benefits of sustained energy delivery from the battery and the high current delivering capability of the supercapacitor bank, it is necessary to obtain information regarding the current drawn by the motors, the gradient at which the vehicle is driving and the mass of the load that needs to be transported. This information is obtained by connecting a shunt current sensor, an accelerometer and a load cell to the vehicle and feeding the information to a microcontroller. Based on these inputs, the microcontroller determines which energy source is best suited for supplying the necessary power to the vehicle.

The microcontroller selected for the implementation of this control system is an Arduino® Mega2560. A combination of 14 PWM, 16 analog and 54 digital pins ensure that the controller has enough capacity to accept and process the sensor inputs. The conceptual design of the energy source management system is shown in Figure 3.

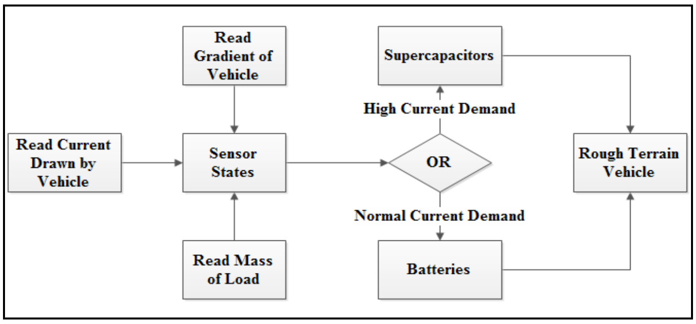

Figure 3: Control system functional flow

A Simulink® model implementing the conceptual design diagram shown in Figure 3 is illustrated in Figure 4. This figure illustrates that if the current drawn by the vehicle exceeds
35 A, the supercapacitor bank is selected to power the rough terrain vehicle. Whenever the current draw drops below the 35 A threshold, the battery is reactivated to power the vehicle. The simulation of this model is shown in the bottom half of Figure 4.

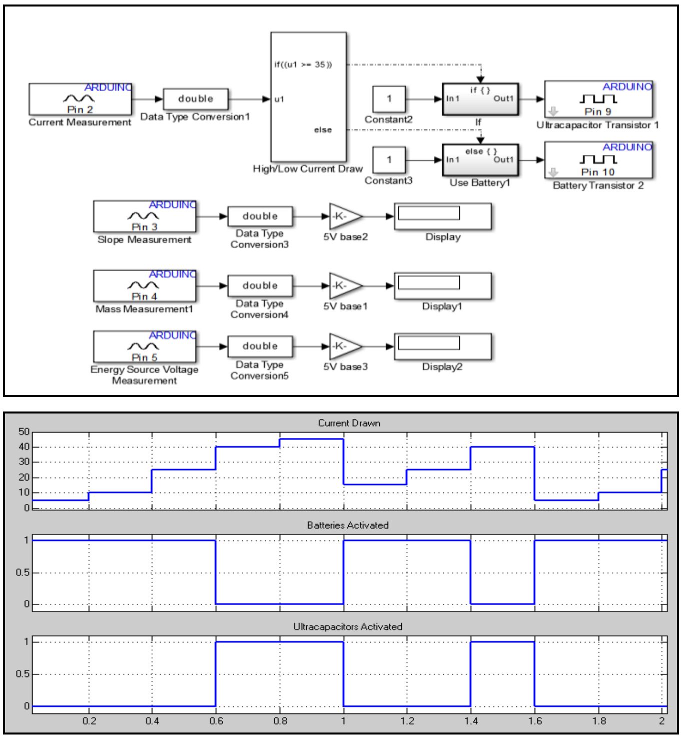

Figure 4:Simulink® battery management control system

C. Speed Control

The speed control of the vehicle is established by an open-loop control configuration as shown in Figure 5.

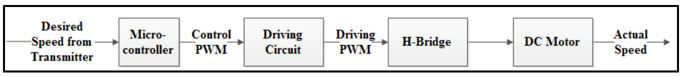

Figure 5: Open-loop speed control

The desired speed of the vehicle is received from a transmitter console operated by the navigator of the vehicle. The desired speed transmitted by the navigator is received by the microcontroller via a RF receiver and the microcontroller outputs a PWM signal according to the desired speed. The PWM signal is fed to a driver circuit which controls the switching of a P and N-channel parallel connected MOSFET H-bridge. The two upper MOSFETs are both P-channel MOSFETs with the two bottom MOSFETs being N-channel. The parallel connected H-bridge shown in Figure 6 allows bidirectional current flow which enables the vehicle to drive forward and backwards.

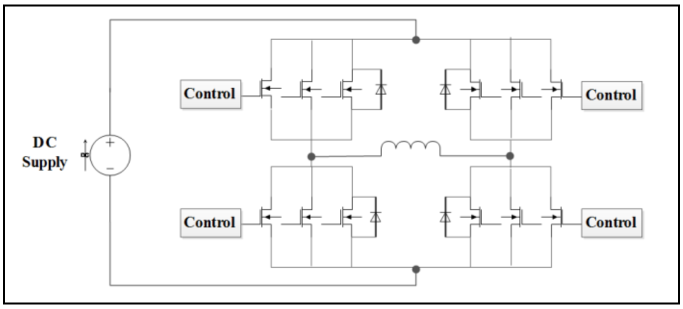

Figure 6: Parallel connected MOSFET H-bridge

The diodes connected across each leg of transistors acts as freewheeling diodes which ensures a path for the current to flow through the motor. These diodes also offer protection against back EMF which is generated when driving inductive loads such as motors.

The H-bridge is designed to safely handle at a current of 50 A. By making use of appropriate calculations and thermal management, a maximum junction temperature of 125 °C is ensured during a continuous current of 50 A.

D. Servo Steering Control

The steering control of the vehicle is performed by creating a closed-loop system as shown in Figure 7 with a high torque DC motor and a potentiometer.

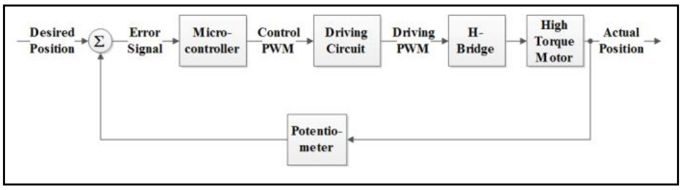

Figure 7: Closed-loop servo control

The desired position is received from the transmitter and the actual position received from the feedback loop is subtracted from the desired position to determine the error signal. The error signal represents the rotational distance between the desired and actual position of the motor's rotor. The error signal is fed to the microcontroller and based on the error signal, the microcontroller outputs a control PWM signal which is fed to the driving circuit and ultimately to an H-bridge similar to the one described in Figure 6. This closed-loop procedure is repeated until the error signal falls within an acceptable range and the motor stops at this position.

E. Rough Terrain Vehicle

The mechanical design of the vehicle must be able to withstand harsh conditions that include excessive temperatures and dusty environments. The design must also be durable and structurally strong enough to carry lightweight tools and materials. The material selected for the construction of the vehicle is steel with a perspex enclosure to house the electrical components. A Solidworks® CAD model of the vehicle is shown in Figure 8.

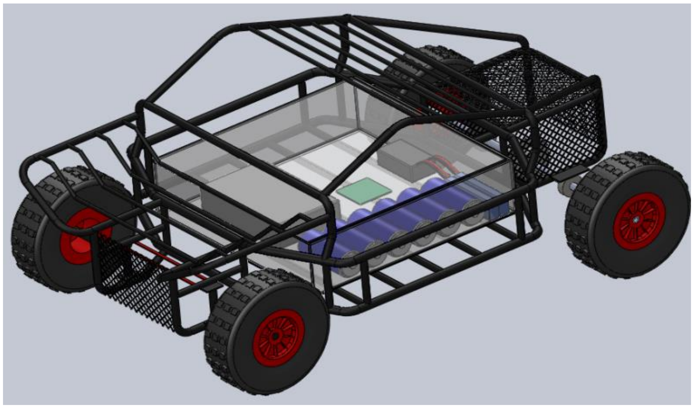

Figure 8: Rough terrain mine vehicle Solidworks® CAD model

F. Sensoring

To determine the current drawn by the vehicle, a shunt current sensor is connected in series with the transistor switching circuit. The current sensor measures the exact amperage drawn by the vehicle and based on these measurements the controller selects the appropriate energy source.

Additional sensors such as an accelerometer, load cell and voltage sensor is connected to the vehicle to gather information regarding the slope at which the vehicle is driving, the mass that is loaded onto the vehicle as well as the voltage level of the energy sources. These sensors all contribute to determining which energy source must be used to power the vehicle.

IV. IMPLEMENTATION AND EVALUATION

A. Battery and Supercapacitor bank discharge time

The running time of the vehicle depends mainly on the loading and driving conditions of the vehicle. If the vehicle is heavily loaded and driving on an incline, a higher current is required to drive the motor which cause the energy source to drain faster. A Simulink® model containing the characteristics of the vehicle's lithium-polymer battery is used to predict the current delivery time of the battery. Figure 9 shows the total discharge time for a certain constant discharge current.

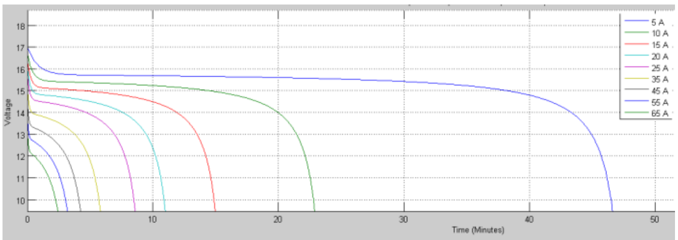

Figure 9: Lithium polymer battery discharge time

A summary of the total discharge times at various loads are shown in Table 2.

Table 2: Battery discharge time at various load currents

Load Current (Ampere)	Continuous Current Delivery Time (Minutes)
4	60
8	30
10	24
15	16
20	12
25	9.5
30	8
35	6.5

The discharge curve of series connected supercapacitor bank is shown in Figure 10, the figure illustrates the supercapacitor bank voltage plotted against time with a constant load current connected to the supercapacitors. The low voltage cut-off level for the supercapacitor bank is at 11.5 V, this is the lowest possible voltage for which it is beneficial to power the 12 V system from the supercapacitor bank.

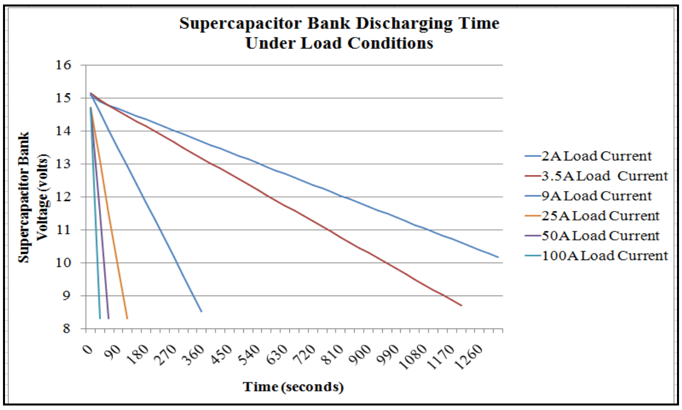

Figure 10: Supercapacitor bank discharge time

From the figure above it is evident that the supercapacitors can supply very high currents for short durations of time. For instance, when a 50 A load is connected to the terminals of the supercapacitors, a continuous current delivery time of about 45 seconds can be expected.

B. *Supercapacitor bank charge times*

The greatest advantage of supercapacitors over batteries is the ability to charge supercapacitors at very high current levels. Figure 11 shows the charging times for numerous values of charging currents.

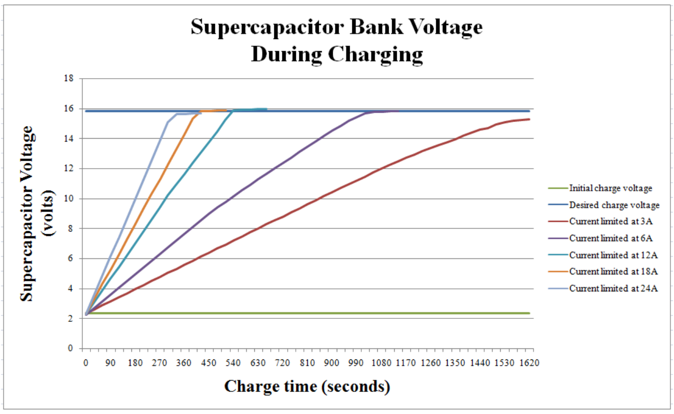

Figure 11: Supercapacitor bank charging time

From the figure above it can be seen that the supercapacitors can be charged at very high current levels. Charging the supercapacitors at 24 A requires only 90 seconds to reach a full state-of-charge when charging from the low-voltage state level. The supercapacitors can be charged at much higher currents and using the graph above to predict the charge time for higher amperage chargers is not difficult. A charger of 50 A will charge the supercapacitor bank within 45 seconds. The charge time of the supercapacitors is in each case governed by the trickle charging at the end of the charging process. The trickle charging is also referred to as top-up charging when the supercapacitor is almost fully charged. The average time required to fully top-up the supercapacitors are about 25% of the total charging time. The supercapacitor bank is shown in Figure 12.

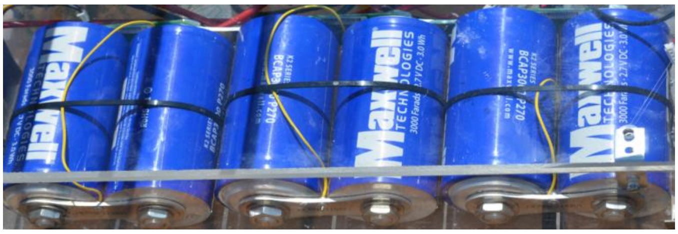

Figure 12: Supercapacitor bank

C. *Arduino® Software Sampling Time*

The time required to switch from the supercapacitor bank to the battery and vice versa is dependent on two variables, namely the power MOSFETs' turn-on/off time and the clock frequency of the microcontroller. The turn-on/off times according to the datasheet is in the order of nanoseconds and it is known that the microcontroller's clock frequency is set at a maximum of 16 MHz. Therefore, the microcontroller speed governs the switching speed between the energy sources. A timing routine has been included in the program code to determine the execution time of the microcontroller and the results are shown in Figure 13.

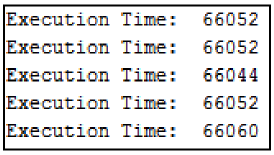
```
Execution Time:  66052
Execution Time:  66052
Execution Time:  66044
Execution Time:  66052
Execution Time:  66060
```

Figure 13: Arduino® Software Execution Time

Therefore, the fastest possible time to read all the sensor data, process the information and perform actions based on these measurements are 66 052 microseconds or 0.06 seconds. Hence, this is the time required to switch between the supercapacitor bank and the battery.

D. *Electronic circuit boards*

The circuit boards for the power electronic speed controller, servo motor controller, energy source management circuit and sensor control board were manufactured as bottom layer circuit boards to reduce manufacturing costs.

The speed controller circuit board is shown in Figure 14 and it can be seen that the implementation corresponds with the design. As shown in the design of the speed controller, there are three MOSFETs connected in parallel to increase the current handling capability.

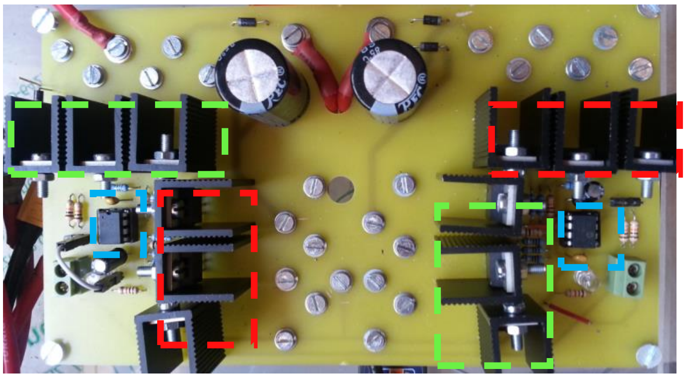

Figure 14: Power electronic speed controller

The blocks indicated in green represents a set of the high-side and low-side MOSFETs, these two legs of the H-bridge is used to turn the drive motor in the forward direction of the vehicle. The red blocks represent the reverse direction of the vehicle. The blue blocks show the MOSFET drivers which receives the input signal from the Arduino® microcontroller and switches the MOSFETs accordingly.

The servo controller is very similar to the speed controller with the exception that only one MOSFET per leg of the H-bridge is used; the circuit board is shown in Figure 15.

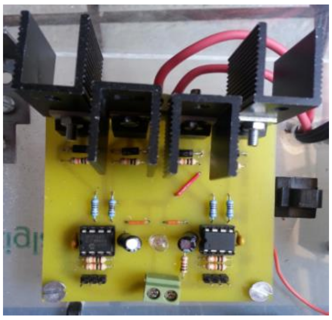

Figure 15: Servo controller

From Figure 15, it can be seen that only four MOSFETs are used with two MOSFET drivers. The energy source management circuit is shown in Figure 16 and contains three MOSFETs with three blocking diodes.

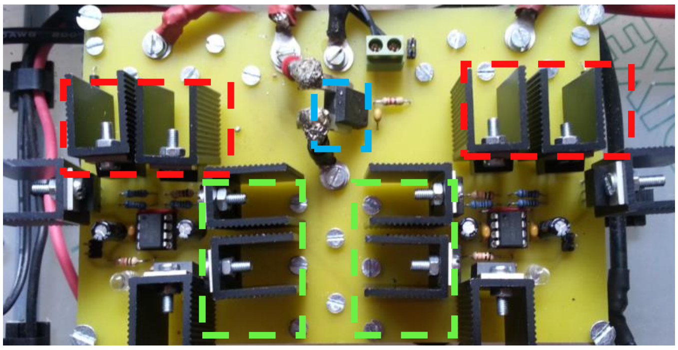

Figure 16: Energy source management circuit

The red blocks show the MOSFETs which is controlled by the MOSFET drivers and the Arduino® microcontroller. The green blocks show the blocking diodes associated with each of the set of the MOSFETs. The blue block shows the current sensor that is used to measure the current drawn by the vehicle.

The sensor control and power board is used to connect all the sensors to a centralized point and to feed the sensor values back to the microcontroller. The board is also used to regulate the voltage of the battery to lower voltage levels which can be used to power the microcontroller and other sensors; the board is shown in Figure 17.

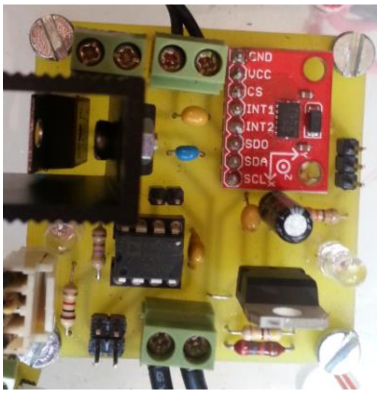

Figure 17: Power and sensor board

The red device shown in the upper right corner of the board is the ADXL345 accelerometer, which is used to read the incline of the vehicle. All of the TO-220 devices are voltage regulators used to step down the voltages to power the sensors and microcontroller.

E. *Drive motor performance test*

The drive motor performance tests are conducted as installed in the vehicle. The test results are performed with the vehicle on level grounds and no mass loaded onto the vehicle; the performance characteristics of the motor at increased throttle intervals are shown in Figure 14.

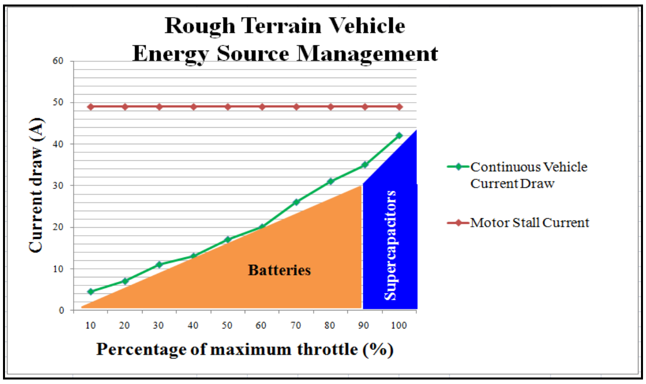

Figure 14: Drive motor performance characteristics

F. *Integrated product test*

The rough terrain vehicle as an integrated product is shown in Figure 15. The vehicle tests were performed in various rough terrain conditions, which include severe inclines and loose gravel.

Figure 15: Integrated product

The driving performance of the vehicle is summarized in Table 3 and shows that a short-fall in the performance of the drive motor exists.

Table 3: Vehicle driving performance

Loaded Mass (Kg)	Incline (Degrees)	Pass/Fail	Current Draw (A)
0	0	Pass	33
0	1	Pass	37
0	2	Pass	39
0	3	Pass	41
0	4	Pass	43
0	5	Fail	48 (Motor stalled)
1	0	Pass	41
2	0	Pass	44
3	0	Fail	48 (Motor stalled)
4	0	Fail	48 (Motor stalled)
5	0	Fail	48 (Motor stalled)

Another test conducted on the vehicle includes the total runtime of the vehicle with the combined energy source of a battery and supercapacitor bank. For the vehicle driving on a random route the sensor data can be used to show a profile containing the incline and current draw of the vehicle. The resultant profile of the route as well as the state of charge of the energy sources is shown in Figure 16.

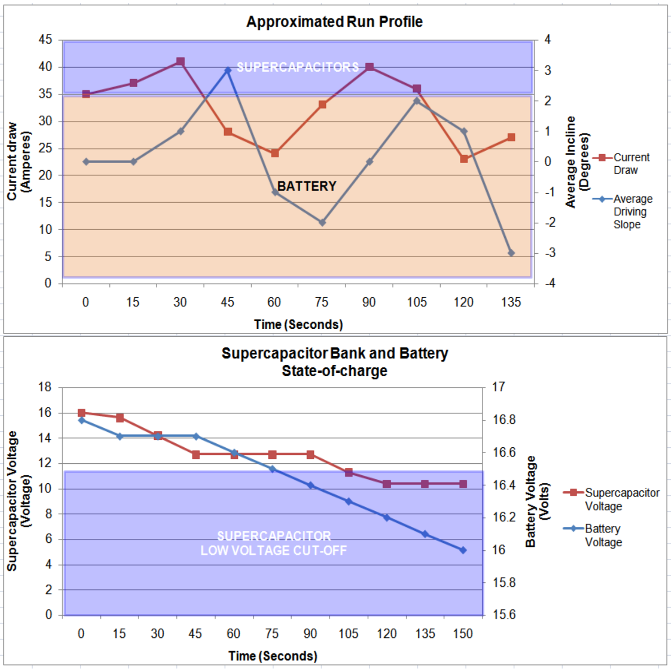

Figure 16: Run profile and energy sources' SOC

From Figure 15, it is clear that the supercapacitor bank must be used very wisely in order to have a sensible energy delivery time. Once the supercapacitor bank is activated to drive the motor, the voltage decreases at a very fast rate. If the voltage level of the supercapacitor bank drops below 11.5 V, the advantages of the supercapacitor bank are eliminated due to the voltage being less than the system's recommended voltage of 12 V. However, the supercapacitor bank can be charged to a full state-of-charge within a few seconds to overcome this shortfall of energy delivery time.

As seen in the run profile of a random route, the low voltage state was reached within two discharge cycles of roughly 40 A of 15 seconds each. After such a discharge, the supercapacitors require a recharge to offer benefits to the vehicle again. The battery's state-of-charge has also dropped by 38 % during the entire run profile. If the vehicle is to continue driving on a similar profile with the supercapacitors recharged, the delivery time of the battery can be predicted to be about 5-6 minutes.

V. CONCLUSION

The supercapacitor rough terrain mine vehicle project was started to research the possibility of implementing supercapacitors in conjunction with a battery as an energy source for an electric vehicle. Supercapacitors are power dense devices, which implies that these devices can deliver a significant amount of current to a load within a very short time. The energy source system implemented in the rough terrain vehicle is powered by a battery and a series connected supercapacitor bank. The goal of the energy source management system is to determine the amount of current drawn by the motors and based on that reading, select the appropriate energy source. By letting the supercapacitor bank supply the vehicle in high current demanding situations, the battery's life can be extended, as the battery does not have to deep cycle to deliver high currents. The energy source testing consisted of determining the charging and discharging capabilities of the battery and the supercapacitor bank. The supercapacitor bank is able to deliver extremely high currents whereas the battery is able to deliver moderately high currents on a continuous basis. The supercapacitors have been tested under severe conditions which include current draws ranging from 3 A to 100 A. When the current drawn is 40 A, similar to average current consumption of the driving motor under heavy load, the expected delivery time of the supercapacitors is about 30 seconds. This is a very short delivery time and therefore the supercapacitors must be used only when the current draw becomes very high.

The integrated test saw the vehicle being taken to a rough terrain, mainly gravel road, and being driven around to determine the run-time of the energy sources, maximum loading conditions as well as the maximum incline at which the vehicle can drive. Due to the shortfall of the driving motor the latter two tests were very restricted not offering satisfactory results. The maximum incline, under no loading, at which the vehicle can drive is 4 degrees. The maximum loading conditions at which the vehicle can drive without much difficulty is with 2 kg loaded onto the vehicle. As for the energy delivery time of the combined energy source, a runtime of about 5-6 minutes is possible. This is mainly due to the fact that the prototype vehicle was fitted with a small Ah battery rating as well as a small supercapacitor bank. The energy delivery time of this bank is about 30-45 seconds when the vehicle's driving motor is under heavy load. By adding more supercapacitor banks in parallel, the overall current delivery time can be increased to a more practical duration; by adding a bank with the exact same specifications will double the current delivery time. Although when considering the financial investment that is required to add several more supercapacitor banks, it is not a viable option considering the much cheaper replacement cost of batteries.

References

[1] Baisden, A.C. & Emadi, A. 2004. ADVISOR-Based Model of a Battery and an Ultra-Capacitor Energy Source for Hybrid Electric Vehicles. Transactions on Vehicular Technology, 53:199-205, January.

[2] Braun, P.V., Cho, J., Pikul, J.H., King, W.P. & Zhang, H. 2012. High power rechargeable batteries. Current Opinion in Solid State and Materials Science, 16(4):186-198, August.

[3] Goldwyer, N. 2007. Mine-specific vehicles spell new direction for technology firm. http://www.miningweekly.com/article/ minespecific-vehicles-spell-new-direction-for-technology-firm-2007-07-20 Date of access: 3 Dec. 2012.

[4] Hitachi. 2012. Datasheet: EH 4000 ACII. http://www.hitachi-c-m.com/za/pdf/products/rigid/eh4000acii/KR-EN030P.pdf Date of access: 3 Dec. 2012.

[5] Maxwell Technologies. 2012. Datasheet: K2 Series Ultracapacitors. http://www.maxwell.com/products/ ultracapacitors/docs/datasheet_k2_series_1015370.pdf Date of access: 3 Dec. 2012.

[6] Neenu, M. 2012. A Battery with Ultracapacitor Hybrid Energy Storage System in Electric Vehicles. International Conference on Advances in Engineering, Science and Management, Nagapattinam, Tamil Nadu, India, 30-31 Mar. Published in the Conference Proceedings, pp. 731-735.

[7] Olivo, T. 2010. Analysis of ultra capacitors as UPS energy storage devices. IEEE SoutheastCon, Concord, NC, 18-21 Mar. Published in the Conference, pp.398-401.

[8] Song, J., Toliyat, A., Tuttle, D. & Kwasinki, A. 2010. A Rapid Charging Station with an Ultracapacitor Energy Storage System for Lug-In Electrical Vehicles. International Conference on Electrical Machines and Systems, Songdo Convensia Incheon, South Korea, 10-13 Oct. Published in the Conference Proceedings, pp. 2003-2007.

[9] Topp, V. 2008. Productivity in the Mining Industry: Measurement and Interpretation. Productivity Commission: Staff Working Paper. Available from SSRN: http://ssrn.com/ abstract=1620243.

[10] Tuite, D. 2012. Get the Low Down on Ultracapacitors. Machine Design, 84(11):48-51, August.